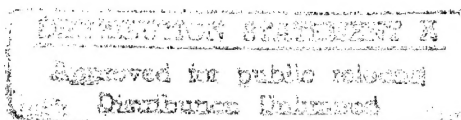NASA Contractor Report 3203

Stress Wave Attenuation in Thin Structures by Ultrasonic Through-Transmission

Samson S. Lee and James H. Williams, Jr.

19960322 084

NASA

PLASTEC 37501

DISCLAIMER NOTICE

UNCLASSIFIED

Technical Report
distributed by

DEFENSE
TECHNICAL
INFORMATION
CENTER

DTIC Acquiring Information-
Imparting Knowledge

Cameron Station
Alexandria, Virginia 22304-6145

UNCLASSIFIED

THIS DOCUMENT IS BEST QUALITY AVAILABLE. THE COPY FURNISHED TO DTIC CONTAINED A SIGNIFICANT NUMBER OF PAGES WHICH DO NOT REPRODUCE LEGIBLY.

NASA Contractor Report 3203

Stress Wave Attenuation in Thin Structures by Ultrasonic Through-Transmission
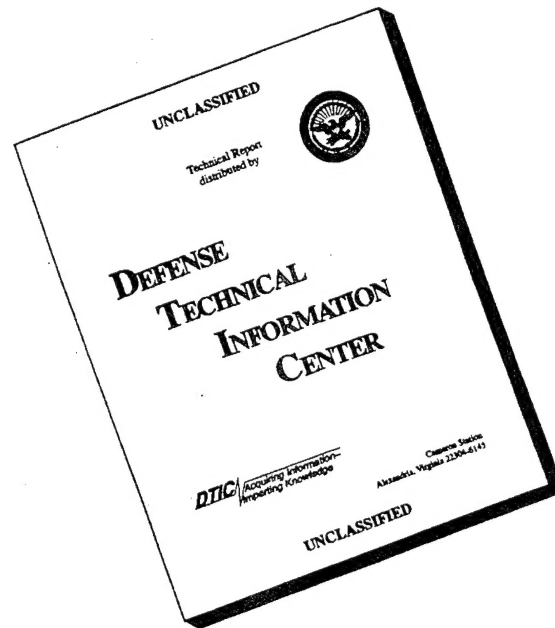
Samson S. Lee and James H. Williams, Jr.
Massachusetts Institute of Technology
Cambridge, Massachusetts

NASA
National Aeronautics
and Space Administration

**Scientific and Technical
Information Office**

1980

INTRODUCTION

Stress wave attenuation denotes the dissipation of the energy of a propagating wave in a medium. Every material is dissipative in this respect and therefore, stress wave attenuation is a constitutive property of the material. The interpretation of stress wave attenuation as a nondestructive evaluation (NDE) technique in the sonic range is as old as the skill of striking a piece of glassware or a metal part and listening for the "characteristic ring of a good specimen". The measurement of stress wave attenuation via ultrasonic NDE is a post-World War II development.

The primary focus of ultrasonic attenuation NDE techniques has been the detection of overt flaws. The concept that such techniques could be used to monitor general structural and material degradation and physical characteristics has received much less attention. In the 1950's Truell and Hikata [1] found that attenuation in aluminum increased with the number of fatigue cycles. More recently, Vary et al. [2-7] have shown that ultrasonic attenuation can be correlated with the mechanical and strength properties of metals, ceramics and fiber composites. In testing graphite fiber polyimide composites, Hayford et al. [8] observed good correlation between the initial attenuation and the shear strength as determined by the short beam shear test. Williams and Doll [9] found that the initial attenuation can be an effective indicator of fatigue life of unidirectional graphite fiber composites subjected to transfiber compression-compression loading.

Ultrasonic attenuation can be measured experimentally by either the pulse-echo technique or the through-transmission technique. In the pulse-echo technique, one or two transducers on the same face of the specimen are used to transmit the pulse and receive its echo from a flaw or the opposite face [8,10,11]. Usually a short duration pulse having a broad-band frequency spectrum is used. Thus, a spectral analysis is required to extract the frequency dependence of the attenuation [12,13]. The through-transmission technique always requires the use of separate transmitting and receiving transducers placed on opposite surfaces of the structure [14-17]. Narrow-band pulses can be used to circumvent the spectral analysis requirement [17]. Through-transmission has the generally recognized disadvantage that when thin sections are tested, the superposition of the transmitted signal with echoes, and even echoes upon echoes, makes any interpretation of the output very difficult.

The through-transmission technique is illustrated in Fig. 1 where the transmitting transducer is driven by a narrow-band frequency wave-packet electrical pulse which has a center frequency ω. Such a signal is shown in the top trace of Fig. 2. A stress wave corresponding to the excitation is introduced into the specimen. The stress wave propagates towards the other transducer and is received as the output signal. A typical output signal is shown in the bottom trace of Fig. 2. (The specimen was a unidirectional graphite fiber epoxy composite (Hercules AS/3501-6), 1.917 cm long

2

with a cross section of 1.080 cm x 1.080 cm. The frequency was 1.2 MHz.) A longitudinal wave was propagated in the x_2 direction which is perpendicular to the fiber and the laminate directions as shown in Fig. 3. A conventional method for determining the stress wave attenuation via the ultrasonic through-transmission technique involves comparing the output signals from two different lengths of otherwise identical specimens. The attenuation $\alpha(\omega)$, which is generally frequency-dependent can be calculated as

$$\alpha(\omega) = \frac{\ln\left(\frac{A_1}{A_2}\right)}{\ell_2 - \ell_1} \tag{1}$$

where the A_i and the ℓ_i are the output signal amplitudes and the lengths of the respective specimens, and ℓn is the natural logarithm.

If the time required for the input pulse to traverse the length of the specimen is much less than the pulse width, the output signal will contain overlapping echo reflections. Such an example is shown in the bottom trace in Fig. 4. (The specimen was the same as that tested in Fig. 2 except that the length was 0.401 cm and the frequency was 0.5 MHz.) The initial portion of the output signal is complicated by both the transient response of the receiver transducer and the superposition of echo reflections while the latter portion of the output signal contains several echo reflections. Thus, the output signal is difficult to interpret in terms of the material attenuation. It is, however, very interesting to note that the output signal settles to a steady-state oscillation. This

3

report describes the use of this easily measured steady-state

output amplitude to determine the attenuation of the specimen.

STEADY-STATE OUTPUT AMPLITUDE ANALYSIS

In the through-transmission technique illustrated in Fig. 1, a sinusoidal electrical signal of voltage amplitude v_i is sent into the transmitting transducer which introduces a propagating stress wave $\sigma_1(x,t)$ given by

$$\sigma_1(x,t) = v_i F_1(\omega) e^{i(kx - \omega t)} \qquad (2)$$

into a nondissipative specimen. The time-varying character of the signal is represented by the complex notation where $i \equiv \sqrt{-1}$ and only the real part of eqn. (3) should be considered. The coordinate x is positive when pointing away from the transmitting transducer and towards the receiving transducer (see Fig. 1), and t is time. The proportionality constant $F_1(\omega)$ is a function of ω and is formally the transduction ratio for the electromechanical gyrating system [18] corresponding to the transformation of an input electrical voltage to a mechanical stress wave in the specimen. $F_1(\omega)$ includes both the characteristics of the transmitting transducer and the stress wave transmissibility of the transducer-specimen interface. The parameter $F_1(\omega)$ has the dimensions of stress per unit voltage. The wave number k is defined by

$$k = \frac{2\pi}{\lambda} \qquad (3)$$

where the wavelength λ is given by

$$\lambda = \frac{C_p(\omega)}{f} \qquad (4)$$

5

and where $C_p(\omega)$ is the phase velocity and f $(f = \frac{\omega}{2\pi})$ is the frequency in Hertz. For wave propagation in a dissipative medium, the stress wave attenuation may be expressed in terms of the attenuation parameter $\alpha(\omega)$, and so eqn. (2) should be replaced by

$$\sigma_1(x,t) = v_i F_1 e^{-\alpha x} e^{i(kx - \omega t)} . \qquad (5)$$

The primary stress wave is defined as the initially propagated stress wave between $x = 0$ and $x = \ell$. The primary stress wave at the end of the specimen $x = \ell$ is given by

$$\sigma_1(\ell,t) = v_i F_1 e^{-\alpha \ell} e^{i(k\ell - \omega t)} . \qquad (6)$$

The electrical output signal from the receiving transducer corresponding to this primary wave is

$$v_1(t) = v_i F_1 F_2 e^{-\alpha \ell} e^{i(k\ell - \omega t - \theta)} \qquad (7)$$

where $\theta(\omega)$ is a phase shift $(0 \leq \theta < 2\pi)$, and the proportionality constant $F_2(\omega)$ is the transduction ratio corresponding to the transformation of a stress wave in the specimen to an output electrical voltage and includes both the characteristics of the receiving transducer and the stress wave transmissibility of the transducer-specimen interface. The parameter $F_2(\omega)$ has the dimensions of voltage per unit stress, and thus the product $F_1(\omega) F_2(\omega)$ is dimensionless.

A portion of the stress wave in eqn. (6) reflects from the end of the specimen with a reflection coefficient $R(\omega)$, $(0 \leq R \leq 1)$,

6

and is given by

$$\sigma_2(x,t) = v_i F_1 R e^{-\alpha(2\ell - x)} e^{i[k(2\ell - x) - \omega t - \phi]} \tag{8}$$

where $\phi(\omega), (0 \le \phi < 2\pi)$, is a phase shift due to the boundary reflection.

The analysis of this process can be continued indefinitely by using the following rules: (1) a stress wave reflected from an end of the specimen can be obtained from the incident stress wave by imposing a phase shift of ϕ and by multiplying the wave amplitude by the reflection coefficient R; and (2) an electrical output signal can be obtained from the stress wave arriving at the receiver end of the specimen by imposing a phase shift of θ and by multiplying the wave amplitude by the parameter F_2. This process is illustrated in Fig. 5.

The steady-state portion of the output signal of the receiving transducer $v_{0,ss}^*$ consists of the transduced portion of the primary stress wave and the transduced portions of all its reflections, and is given by

$$v_{0,ss}^* = v_i F_1 F_2 e^{-\alpha\ell} e^{i(k\ell - \omega t - \theta)} + v_i F_1 F_2 R^2 e^{-3\alpha\ell} e^{i(3k\ell - \omega t - 2\phi - \theta)}$$

$$+ v_i F_1 F_2 R^4 e^{-5\alpha\ell} e^{i(5k\ell - \omega t - 4\phi - \theta)} + \ldots$$

$$= v_i F_1 F_2 \sum_{j=0}^{\infty} R^{2j} e^{-(2j+1)\alpha\ell} e^{i[(2j+1)k\ell - \omega t - 2j\phi - \theta]} . \tag{9}$$

7

If the signal represented by eqn. (9) is phase-shifted by an amount $(k\ell - \theta)$, the phase-shifted steady-state output $v_{0,ss}$ becomes

$$v_{0,ss} = v_i F_1 F_2 \sum_{j=0}^{\infty} R^{2j} e^{-(2j+1)\alpha\ell} e^{i[2j(k\ell - \phi) - \omega t]} . \quad (10)$$

No generality is lost by using eqn. (10) instead of eqn. (9) because the exact phase information of the output signal is not used. By defining

$$\phi'(\omega) = k\ell - \phi , \quad (11)$$

eqn. (10) can be rewritten as

$$v_{0,ss} = v_i F_1 F_2 \sum_{j=0}^{\infty} R^{2j} e^{-(2j+1)\alpha\ell} e^{i(2j\phi' - \omega t)} . \quad (12)$$

Considering only the real part of eqn. (12) gives

$$v_{0,ss} = v_i F_1 F_2 e^{-\alpha\ell} \sum_{j=0}^{\infty} R^{2j} e^{-2j\alpha\ell} \cos(2j\phi' - \omega t) . \quad (13)$$

Eqn. (13) can be manipulated to give

$$v_{0,ss} = v_i F_1 F_2 e^{-\alpha\ell} \left[\cos\omega t \sum_{j=0}^{\infty} e^{-j(2\alpha\ell - 2\ell nR)} \cos[j(2\phi')] \right.$$

$$\left. + \sin\omega t \sum_{j=0}^{\infty} e^{-j(2\alpha\ell - 2\ell nR)} \sin[j(2\phi')] \right] . \quad (14)$$

8

The summations in eqn. (14) can be summed exactly to [19]*

$$v_{0,ss} = v_i F_1 F_2 e^{-\alpha\ell} \left\{ \cos\omega t \left[1 + \frac{1}{2} \left[\frac{\sinh(2\alpha\ell - 2\ell nR)}{\cosh(2\alpha\ell - 2\ell nR) - \cos(2\phi')} - 1 \right] \right] \right.$$

$$\left. + \sin\omega t \left[\frac{1}{2} \frac{\sin(2\phi')}{\cosh(2\alpha\ell - 2\ell nR) - \cos(2\phi')} \right] \right\}$$

which can be rewritten as

$$v_{0,ss} = \frac{v_i F_1 F_2 e^{-\alpha\ell}}{2\{\cosh[2(\alpha\ell - \ell nR)] - \cos(2\phi')\}} \left[e^{2(\alpha\ell - \ell nR)} \cos\omega t \right.$$

$$\left. - \cos\omega t \cos(2\phi') + \sin\omega t \sin(2\phi') \right] . \tag{15}$$

Extrema of $v_{0,ss}$ can be obtained by using

$$\frac{dv_{0,ss}}{dt} = 0 . \tag{16}$$

---

*The useful equations are

$$\sum_{n=0}^{\infty} e^{-n\gamma} \sin(n\delta) = \frac{1}{2} \frac{\sin\delta}{\cosh\gamma - \cos\delta} , \quad \gamma > 0$$

$$1 + 2 \sum_{n=0}^{\infty} e^{-n\gamma} \cos(n\delta) = \frac{\sinh\gamma}{\cosh\gamma - \cos\delta} , \quad \gamma > 0$$

Note that because $(2\alpha\ell - 2\ell nR) > 0$, these relations are appropriate for the desired summations.

9

Substitution of eqn. (15) into eqn. (16) gives

$$\frac{\sin\omega t}{\cos\omega t} = \tan\omega t = \frac{\sin(2\phi')}{e^{2(\alpha\ell - \ell nR)} - \cos(2\phi')} \quad . \quad (17)$$

Noting that $\dfrac{1}{\cos^2\theta} = 1 + \tan^2\theta$, eqn. (17) can be rewritten as

$$\cos\omega t = \frac{1}{\sqrt{1 + \left[\dfrac{\sin(2\phi')}{e^{2(\alpha\ell - \ell nR)} - \cos(2\phi')}\right]^2}} \quad . \quad (18)$$

Substitution of eqns. (17) and (18) into eqn. (15) and manipulation
of the resulting expression give the amplitude of the steady-state
output as

$$\max v_{0,ss} = \frac{v_i F_1 F_2 e^{-\alpha\ell} \sqrt{e^{4(\alpha\ell - \ell nR)} - 2\cos(2\phi')e^{2(\alpha\ell - \ell nR)} + 1}}{2\{\cosh[2(\alpha\ell - \ell nR)] - \cos(2\phi')\}} \quad . \quad (19)$$

A strategy for using eqn. (19) to determine the attenuation of
materials from the measured through-transmission steady-state output
amplitude will be illustrated in the next section.

10

EXAMPLE OF APPLICATION

If the parameters $F_1(\omega)F_2(\omega)$, $R(\omega)$ and $\phi(\omega)$ are known, the attenuation $\alpha(\omega)$ can be determined from eqn. (19) and the experimentally measured steady-state output amplitude. Note also that the phase velocity $C_p(\omega)$ is required for calculating the wave number k.

In general, the required parameters can be measured a priori by testing different lengths of otherwise identical specimens. For each frequency of interest the phase velocity, $C_p(\omega)$, and the parameters $\alpha(\omega)$, $F_1(\omega)F_2(\omega)$, $R(\omega)$ and $\phi(\omega)$ can be found in that order based on the experimental data. Then, $C_p(\omega)$, $F_1(\omega)F_2(\omega)$, $R(\omega)$ and $\phi(\omega)$ can be assumed constant for future tests on the material where the specimens have the same cross section but any length. An example demonstrating these calculations for some graphite fiber epoxy composite samples follows.

The material was a unidirectional graphite fiber epoxy composite (Hercules AS/3501-6). The specimens were rods with a square cross section, 1.080 cm (0.425 in) on a side as shown in Fig. 3. The lengths of the specimens were 0.401 cm (0.158 in), 0.662 cm (0.261 in), 1.086 cm (0.427 in), 1.278 cm (0.503 in), 1.917 cm (0.755 in), 2.545 cm (1.002 in), 3.797 cm (1.495 in) and 5.093 cm (2.005 in). The direction of longitudinal wave propagation was perpendicular to both the fiber and the laminate directions and is indicated in Fig. 3 as the x_2 direction. The experimental

11

system is shown in Fig. 6. The transducers were Acoustic Emission Technology (AET) FC-500 transducers and the couplant was AET SC-6. The peak-to-peak input voltage to the transmitting transducer was 280 volts. A pressure of 0.3 MN/m^2 (44 psi) was applied to the transducer-specimen interface through the spring scales. As shown in [17], this pressure exceeded the "saturation pressure", which is defined as the minimum interface pressure that results in the maximum output signal amplitude, all other parameters being held constant. The frequency range was 0.3 - 3MHz.

The wave group velocity C_g was determined by

$$C_g(\omega) = \frac{\ell_2 - \ell_1}{t_2 - t_1} \tag{20}$$

where t_i are the wave packet transit times in the respective specimen lengths ℓ_i. The experimentally measured group velocity is independent of frequency and is equal to 2.82×10^5 cm/sec (1.11×10^5 in/sec). Because the group velocity is independent of frequency, the composite material is nondispersive, and thus the group velocity is equal to the phase velocity. Using sufficiently long specimens in order to achieve nonoverlapping pulses such as depicted in Fig. 2, the attenuation $\alpha(\omega)$ of the material was calculated from the amplitudes of the primary stress wave output signals using eqn. (1) and is plotted in Fig. 7.

The parameter $F_1(\omega)F_2(\omega)$ can be obtained from the amplitude of the primary stress wave output signal also. Considering only

the amplitude of the signal in eqn. (7) and rearranging eqn. (7) give

$$F_1(\omega) F_2(\omega) = \frac{v_1}{v_i} e^{\alpha l} .$$ (21)

Using the attenuation plot in Fig. 7 and the experimental values of v_1 and v_i, the resulting $F_1(\omega) F_2(\omega)$ can be plotted as shown in Fig. 8.

In order to determine the reflection coefficient $R(\omega)$, it is necessary to measure the first reflection amplitude $v_{reflect}$ from the output signal when the second reflection amplitude is negligible. Such a situation is illustrated in Fig. 9 where the length of the specimen was 1.086 cm. The amplitude of the first reflection $v_{reflect}$ as indicated in Fig. 5 is

$$v_{reflect} = v_i F_1 F_2 R^2 e^{-3\alpha l}.$$ (22)

Rearranging eqn. (22) gives the reflection coefficient

$$R(\omega) = \sqrt{\frac{v_{reflect}}{v_i F_1 F_2 e^{-3\alpha l}}} .$$ (23)

Again, note that in accordance with energy conservation, the reflection coefficient is subject to the restriction $0 \le R \le 1$. Using Figs. 7 and 8 and the experimental values of $v_{reflect}$ and v_i, the resulting $R(\omega)$ can be computed and is shown in Fig. 10.

The phase shift parameter $\phi(\omega)$ can be determined from eqn. (19) based on the steady-state output amplitude. Good accuracy can be achieved if the steady-state output consists of sizable reflections such that the primary stress wave does not dominate the output signal. Using the curves in Figs. 7, 8 and 10, a value of $\cos(2\phi')$ can be obtained from the steady-state output amplitude and eqn. (19) by trial and error. The phase shift ϕ can then be computed from the arc cosine and eqn. (11). However, because

$$\cos^{-1}(2\phi') = \cos^{-1}(2\pi - 2\phi') , \qquad (24)$$

these calculations result in two different values for ϕ' and thus ϕ. Substitution of the two values of ϕ into eqn. (19) to compute the steady-state output amplitude for a different length specimen and comparison of the computed value with the experimental value will select the correct ϕ. The resulting phase shift parameter $\phi(\omega)$ is plotted in Fig. 11.

With the use of Figs. 8, 10 and 11, it is possible to compute the attenuation $\alpha(\omega)$ from eqn. (19) by measuring the steady-state output amplitude from any length (thickness) specimen of the material assuming that the same equipment, specimen cross section and direction of longitudinal wave propagation are maintained. Of course, the assumption is that the phase velocity and the parameters $F_1(\omega) F_2(\omega)$, $R(\omega)$ and $\phi(\omega)$ remain invariant with specimen substitution. It has been shown [9] that the phase velocity when

14

compared with the attenuation is relatively insensitive to the fatigue state of Hercules AS/3501-6. Further, if the surface condition is consistent from specimen to specimen, the parameters $F_1(\omega)F_2(\omega)$, $R(\omega)$ and $\phi(\omega)$ are expected to remain significantly invariant.

CONCLUSIONS

The steady-state output amplitude of an ultrasonic through-transmission measurement has been analyzed and the result has been given in closed form. Assuming that a set of similar specimens of the same cross section can be tested a priori in the same wave mode in order to tabulate values of the product of the input and output transduction ratios $(F_1(\omega)F_2(\omega))$, the specimen-transducer reflection coefficient $(R(\omega))$, the specimen-transducer phase shift parameter $(\phi(\omega))$, and the material phase velocity $(C_p(\omega))$, the attenuation $\alpha(\omega)$ for future specimens can be determined from the steady-state output amplitude and eqn. (19).

The steady-state output amplitude has the advantage of being easily measurable. Because echo reflections are actually accounted for, there is no need to avoid overlapping echoes in the output signal and thus there is no apparent limitation on the minimum length or thickness of the specimen. An additional advantage of using the steady-state output amplitude is that once Figs. 8, 10 and 11 have been obtained, further testing does not require the more specialized pulse oscillator or a spectrum analyzer because a simple harmonic signal generator is sufficient.

16

REFERENCES

1. R. Truell and A. Hikata, "Fatigue and Ultrasonic Attenuation", Symposium on Nondestructive Testing, Los Angeles, Calif., Sept. 17 and 18, 1956, American Society for Testing Materials, ASTM STP No. 213, Philadelphia, Penn., 1957, pp. 63-69.

2. A. Vary and K. J. Bowles, "Ultrasonic Evaluation of the Strength of Unidirectional Graphite-Polyimide Composites", NASA Technical Memorandum TM-73646, April, 1977.

3. A. Vary and K. J. Bowles, "Use of an Ultrasonic-Acoustic Technique for Nondestructive Evaluation of Fiber Composite Strength", NASA Technical Memorandum TM-73813, Feb., 1978.

4. A. Vary and R. F. Lark, "Correlation of Fiber Composite Tensile Strength with the Ultrasonic Stress Wave Factor", NASA Technical Memorandum TM-78846, April, 1978.

5. A. Vary, "Correlations among Ultrasonic Propagation Factors and Fracture Toughness Properties of Metallic Materials", Materials Evaluation, vol. 36, no. 7, June 1978, pp. 55-64.

6. A Vary, "Quantitative Ultrasonic Evaluation of Mechanical Properties of Engineering Materials", NASA Technical Memorandum TM-78905, June, 1978.

7. A. Vary, "Correlations Between Ultrasonic and Fracture Toughness Factors in Metallic Materials", NASA Technical Memorandum TM-73805, June, 1978.

8. D. T. Hayford, E. G. Henneke, II, and W. W. Stinchcomb, "The Correlation of Ultrasonic Attenuation and Shear Strength in Graphite-Polyimide Composites", Journal of Composite Materials, Vol. 11, Oct., 1977, pp. 429-444.

9. J. H. Williams, Jr. and B. Doll, "Ultrasonic Attenuation as an Indicator of Fatigue Life of Graphite/Epoxy Composites", NASA CR-3179, 1979.

10. J. Krautkramer and H. Krautkramer, Ultrasonic Testing of Materials, Second Edition, Springer-Verlag, N.Y., 1977.

11. E. P. Papadakis, "Ultrasonic Attenuation in Thin Specimens Driven Through Buffer Rods", The Journal of the Acoustical Society of America, vol. 44, no. 3, 1968, pp. 724-734.

12. E. P. Papadakis, K. A. Fowler and L. C. Lynnworth, "Ultra-sonic Attenuation by Spectrum Analysis of Pulses in Buffer Rods: Method and Diffraction Corrections", The Journal of the Acoustical Society of America, vol. 53, no. 5, 1973, pp. 1336-1343.

13. A Vary, "Computer Signal Processing for Ultrasonic Attenuation and Velocity Measurements for Material Property Characterizations", NASA Technical Memorandum TM-79180, April, 1979.

14. H. J. Sutherland and R. Lingle, "Geometric Dispersion of Acoustic Waves by a Fibrous Composite", Journal of Composite Materials, vol. 6, Oct., 1972, pp. 490-502.

15. H. J. Sutherland, "Dispersion of Acoustic Waves by Fiber-Reinforced Viscoelastic Materials", The Journal of the Acoustical Society of America, vol. 57, no. 4, 1975, pp. 870-875.

16. S. Serabian, "Influence of Attenuation Upon the Frequency Content of a Stress Wave Packet in Graphite," The Journal of the Acoustical Society of America, vol. 42, no. 5, 1967, pp. 1052-1059.

17. J. H. Williams, Jr., N. Nayeb-Hashemi and S. S. Lee, Ultra-sonic Attenuation and Velocity in AS/3501-6 Graphite/Epoxy Fiber Composite", NASA CR-3180, 1979.

18. J. L. Shearer, A. T. Murphy and H. H. Richardson, Introduction to System Dynamics, Addison-Wesley Publishing Co., Reading, Mass., 1967, p. 94.

19. I. S. Gradshteyn and I. M. Ryzhik, Table of Integrals, Series, and Products, Academic Press, N.Y., 1965, p. 42.
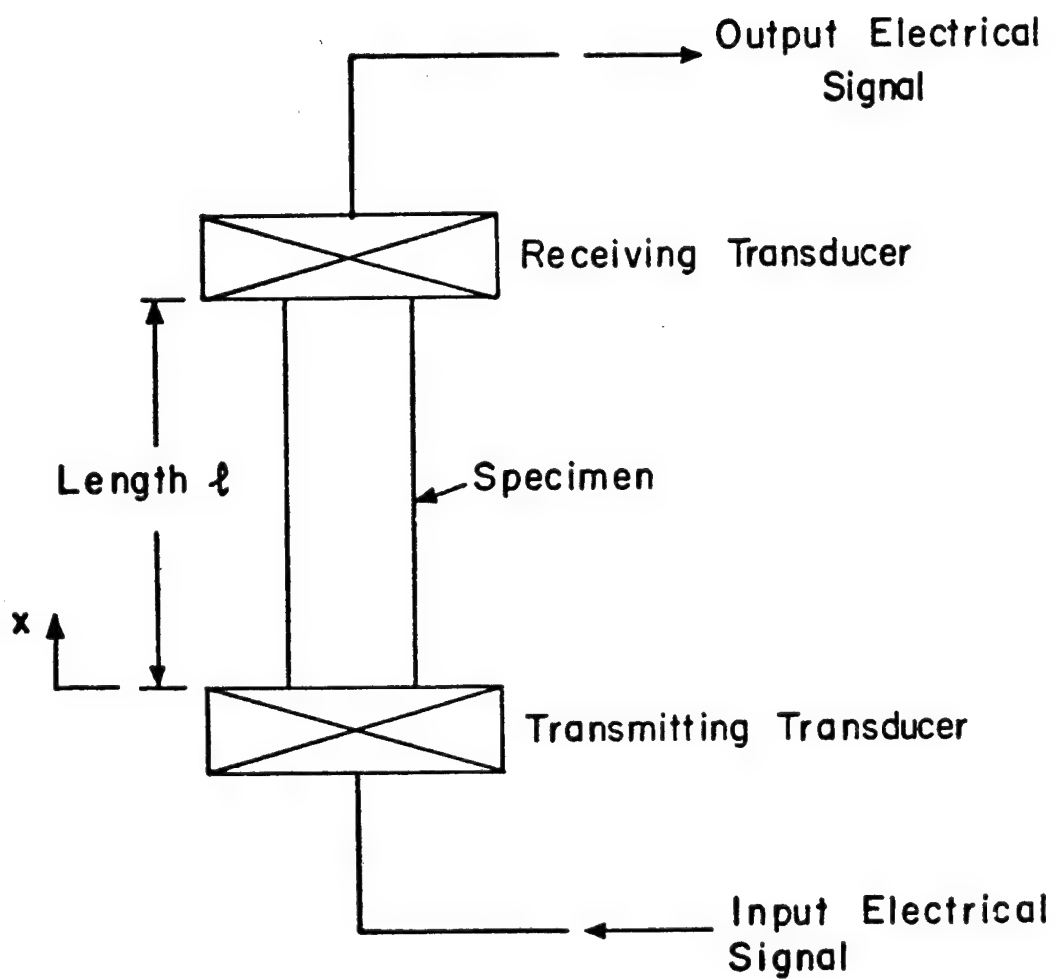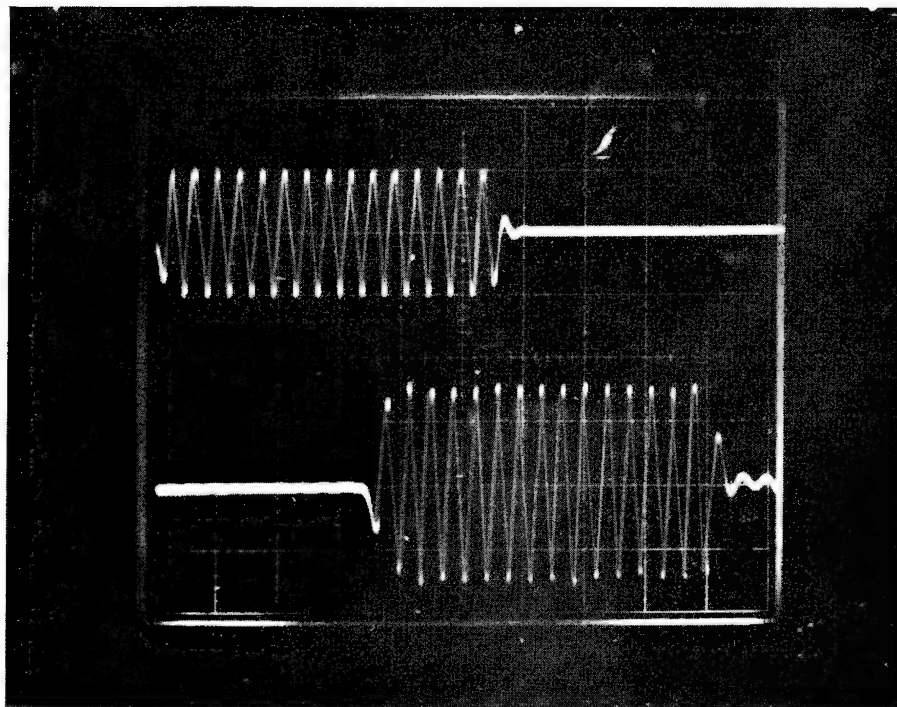
Fig. 1   Schematic of specimen and transducers in
ultrasonic through-transmission testing.

19

Top trace: Input signal to the transmitting transducer
             Scale = 5v/Large Div.
             (The signal was attenuated 29dB before
             displaying.)

Bottom trace: Output signal from the receiving transducer
                Scale = 0.1v/Large Div.

Time scale: 2µs/Large Div.

Frequency: 1.2 MHz

Fig. 2   Typical ultrasonic through-transmission input
         and output signals with no echo superposition.
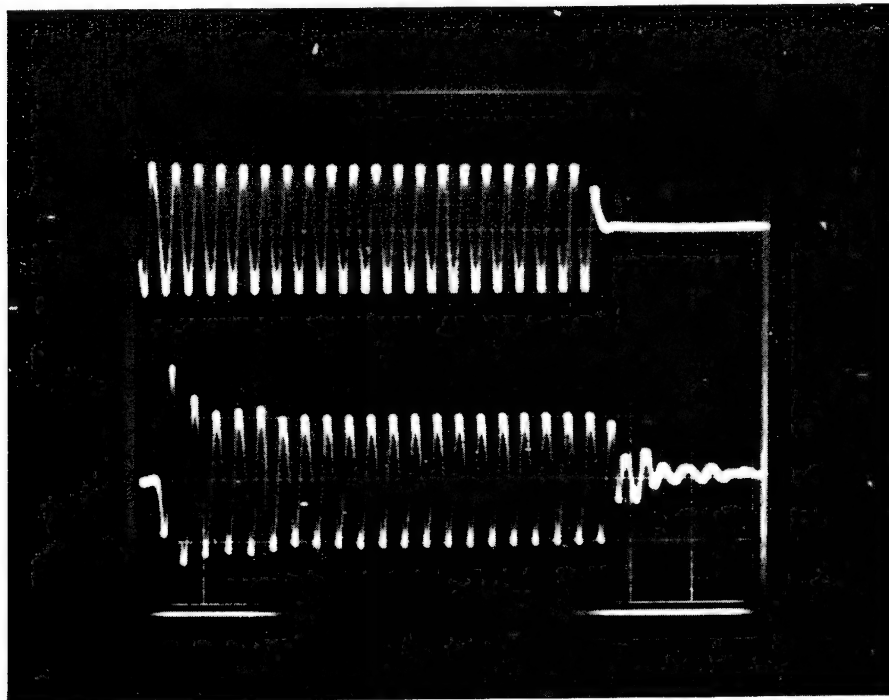
20
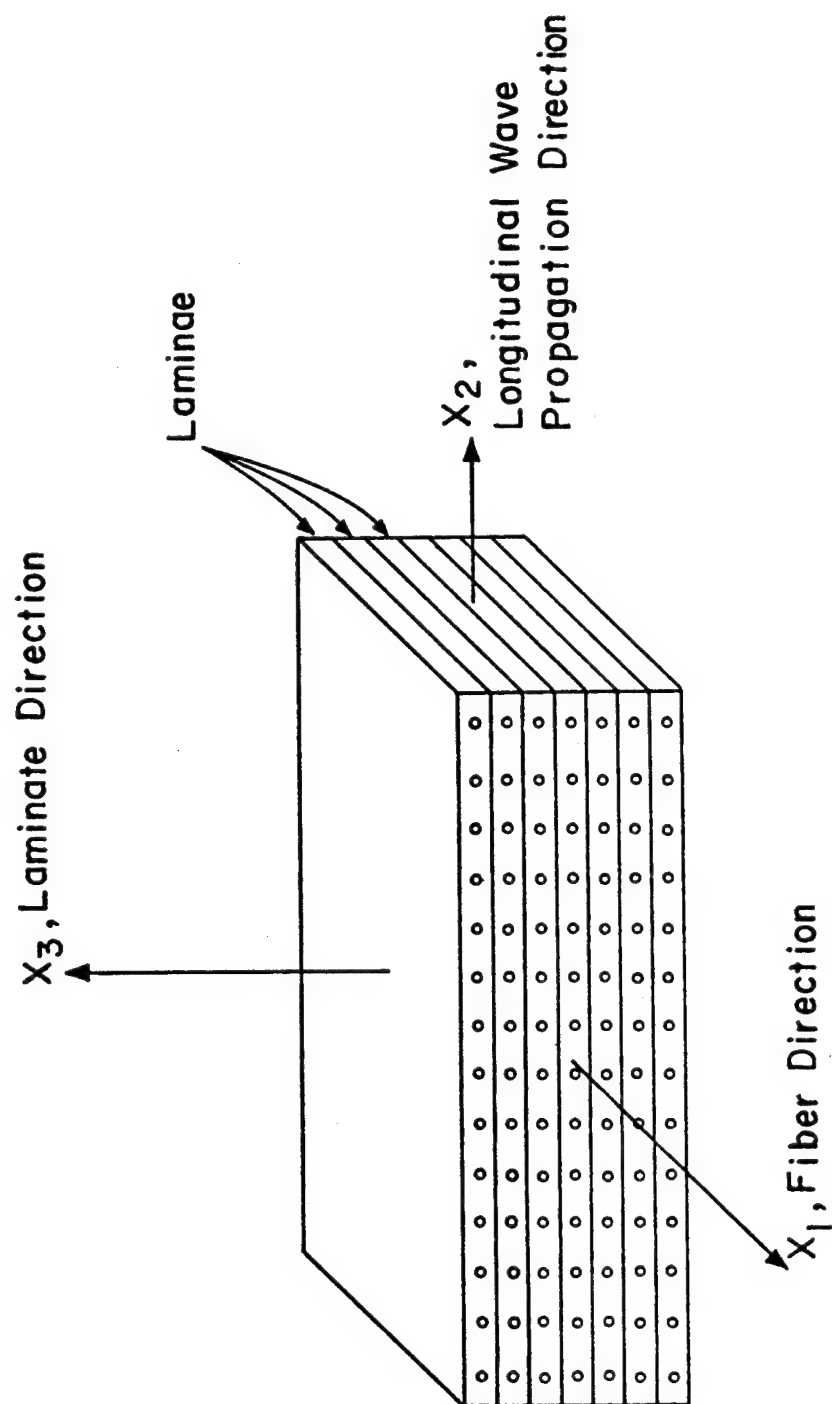
Fig. 3   Schematic of composite laminate showing principal axes including wave propagation direction.

Top trace: Input signal to the transmitting transducer
              Scale = 5v/Large Div.
              (The signal was attenuated 29dB before
              displaying.)

Bottom trace: Output signal from the receiving transducer
              Scale = 0.2v/Large Div.

Time scale: 5µs/Large Div.

Frequency: 0.5 MHz

Fig. 4   Typical signals in ultrasonic through-transmission
          testing showing the complicated output waveform due
          to transients and multiple reflections and showing
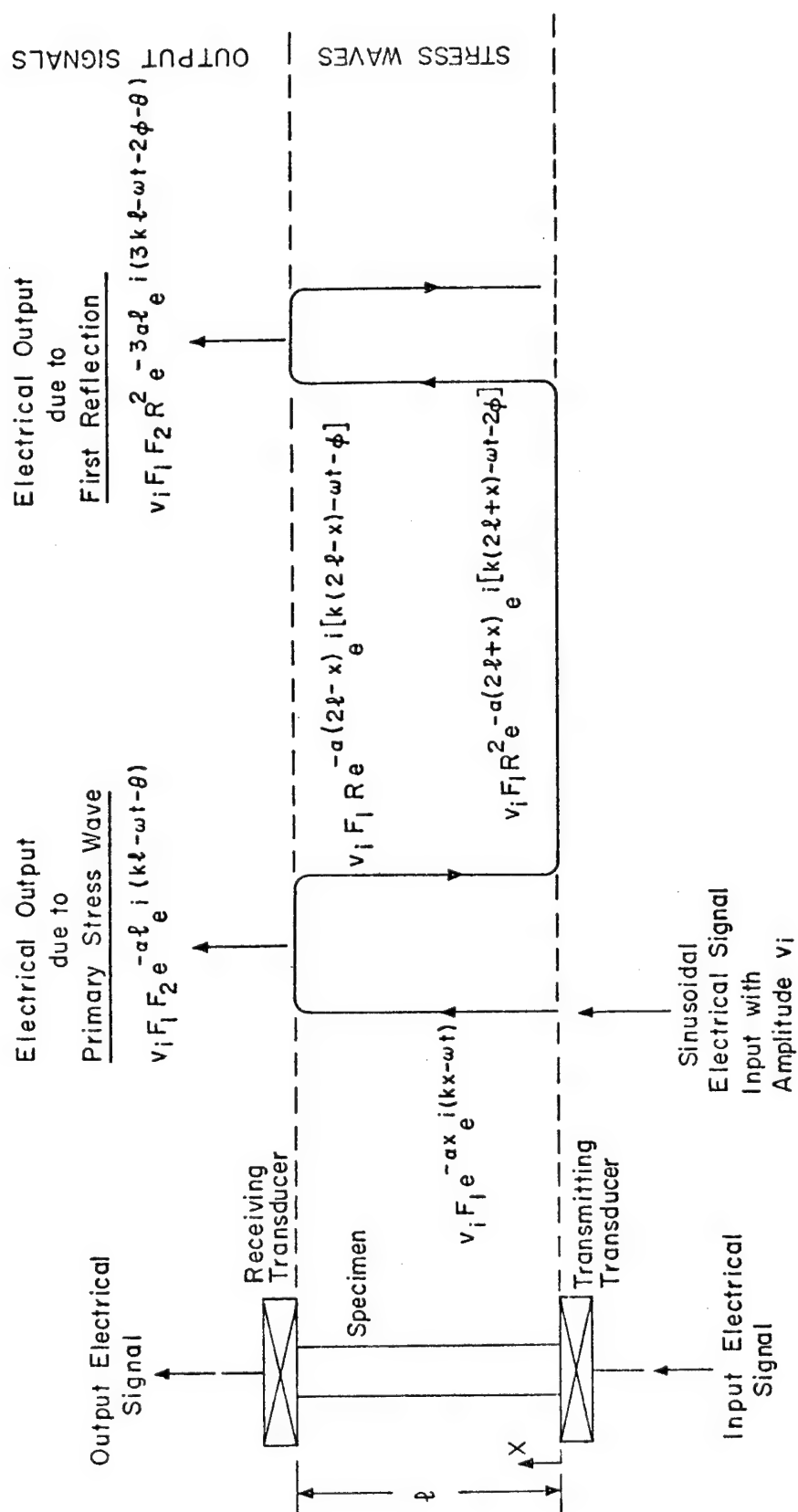   the eventual steady-state amplitude.

22

OUTPUT SIGNALS | STRESS WAVES

Electrical Output
due to
First Reflection

$$v_i F_1 F_2 R^2 e^{-3a\ell} e^{i(3k\ell - \omega t - 2\phi - \theta)}$$

Electrical Output
due to
Primary Stress Wave

$$v_i F_1 F_2 e^{-a\ell} e^{i(k\ell - \omega t - \theta)}$$

$$v_i F_1 R e^{-a(2\ell - x)} e^{i[k(2\ell - x) - \omega t - \phi]}$$

$$v_i F_1 R^2 e^{-a(2\ell + x)} e^{i[k(2\ell + x) - \omega t - 2\phi]}$$

$$v_i F_1 e^{-ax} e^{i(kx - \omega t)}$$

Sinusoidal
Electrical Signal
Input with
Amplitude v_i

Receiving
Transducer

Transmitting
Transducer

Specimen

Output Electrical
Signal

Input Electrical
Signal

X

ℓ

Fig. 5   Illustration showing propagating stress wave and corresponding output signal.
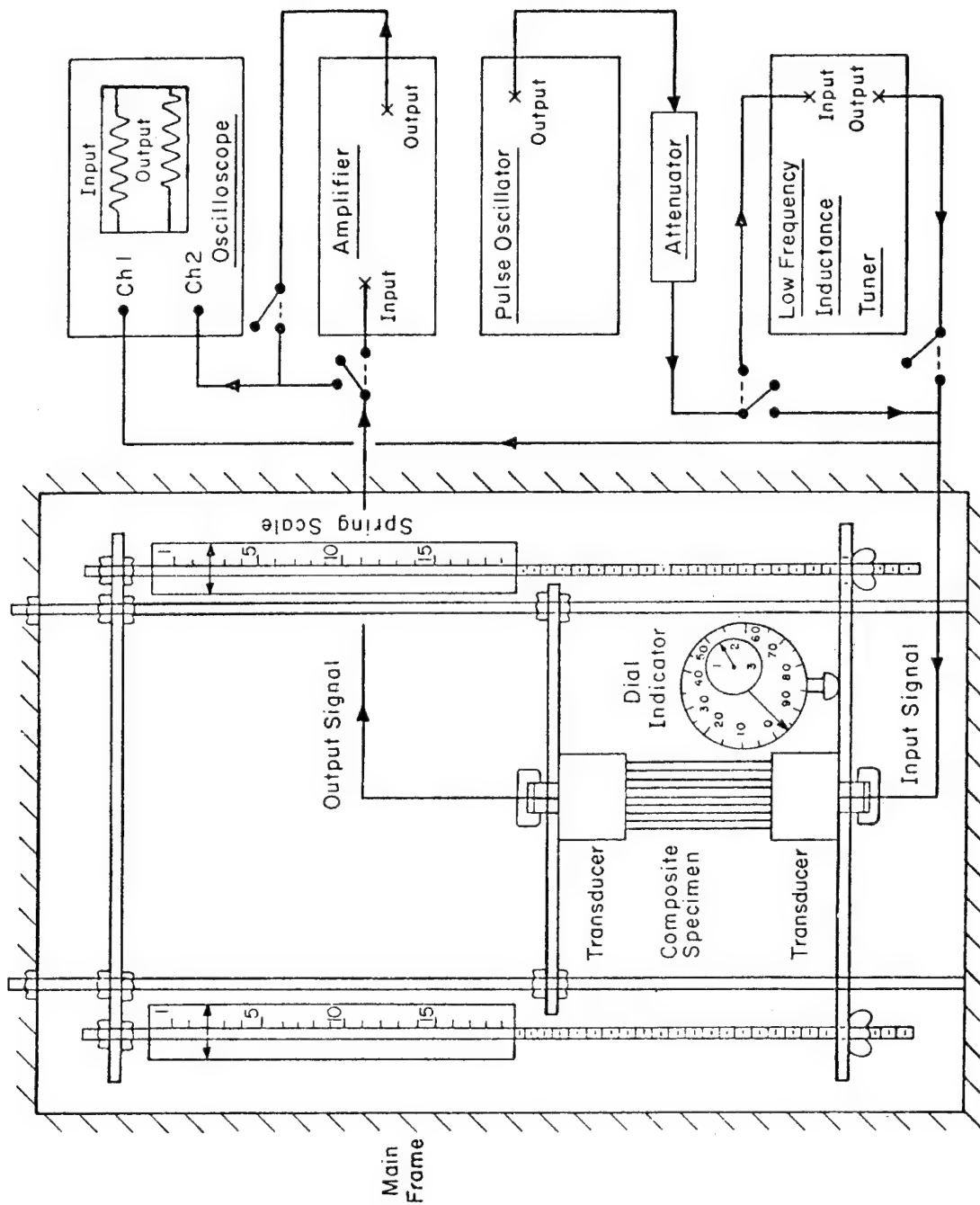
Fig. 6   Schematic of experimental system.
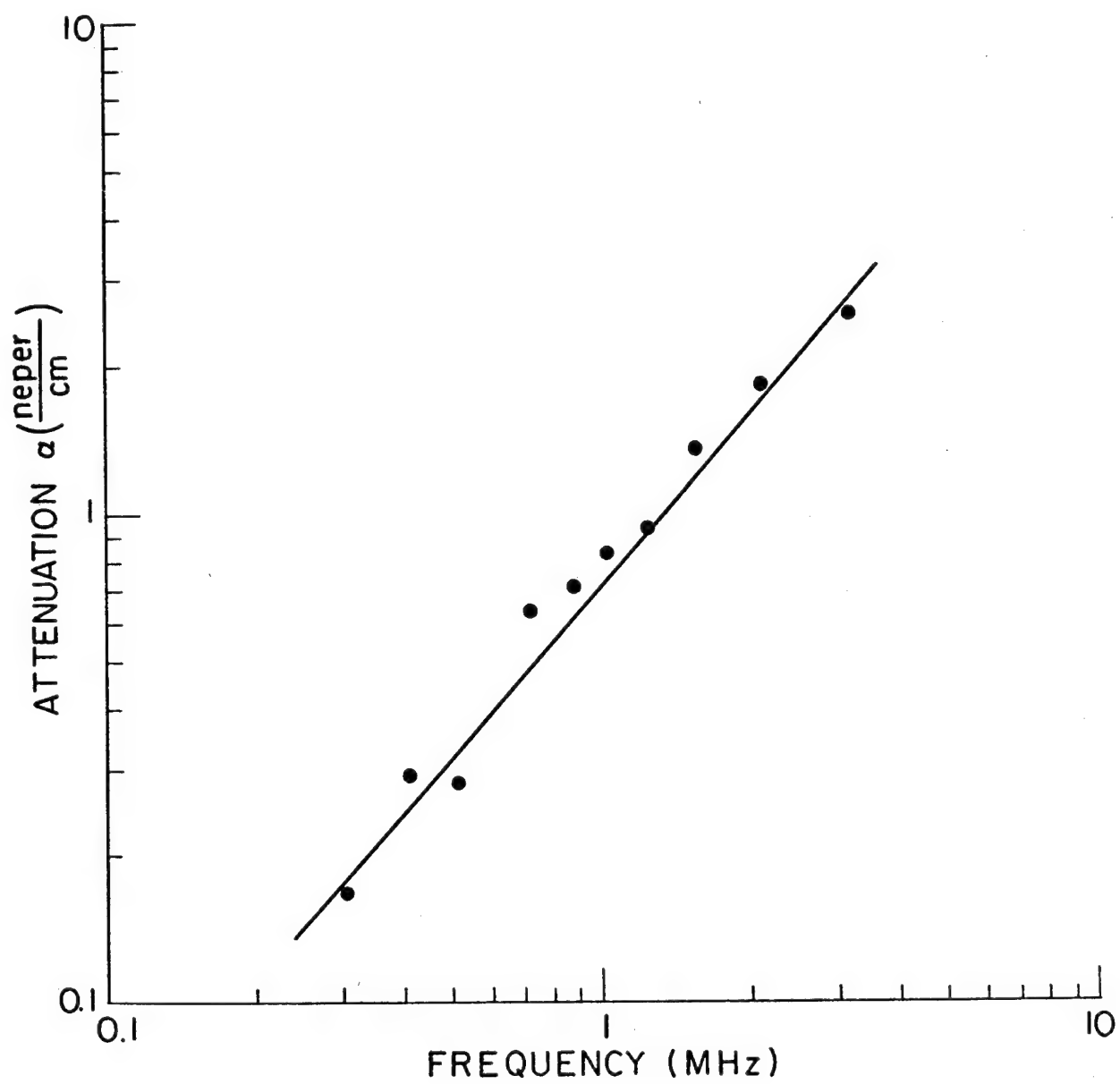
24

Fig. 7   Attenuation $\alpha(\omega)$ of composite for longitudinal wave propagation in
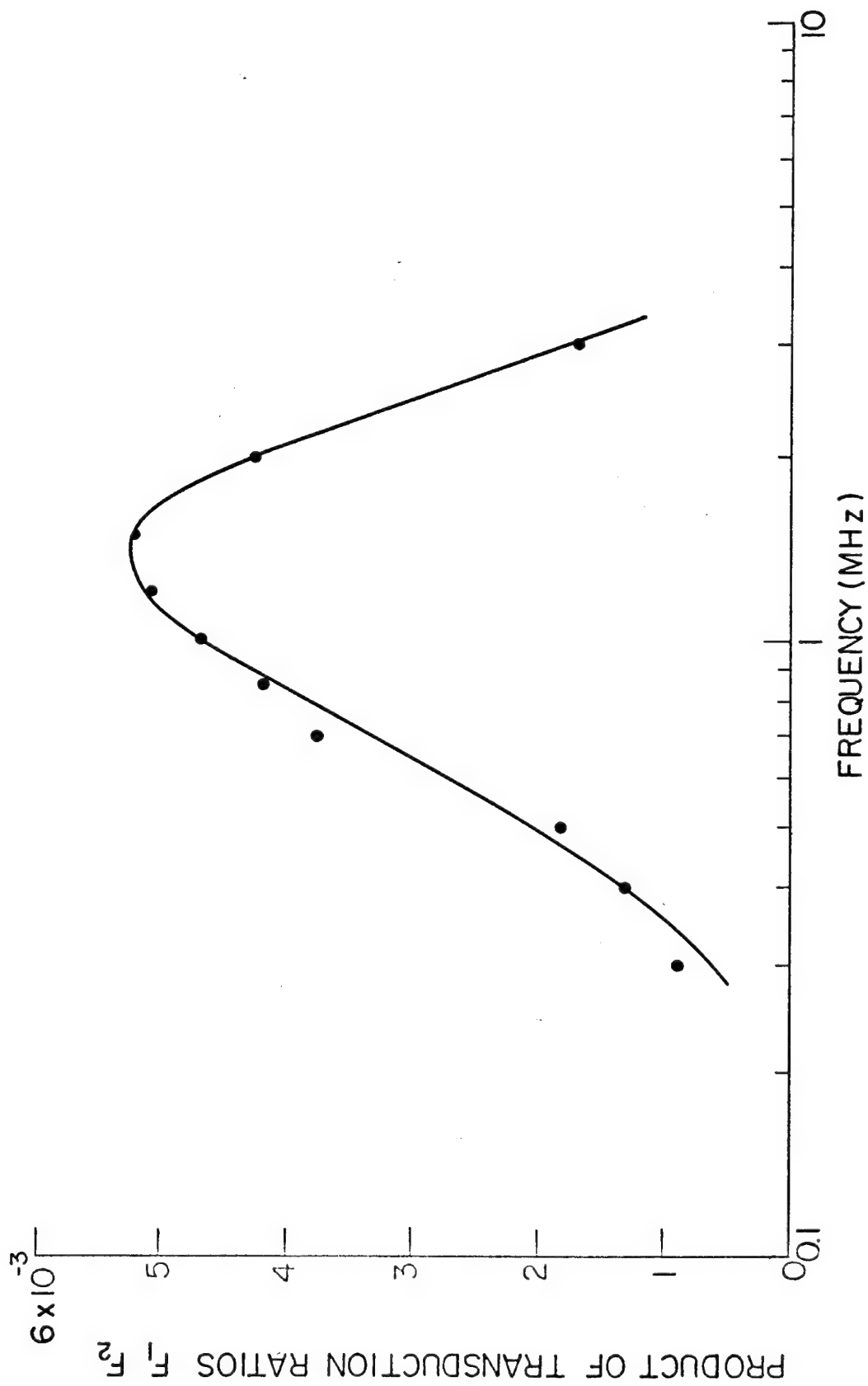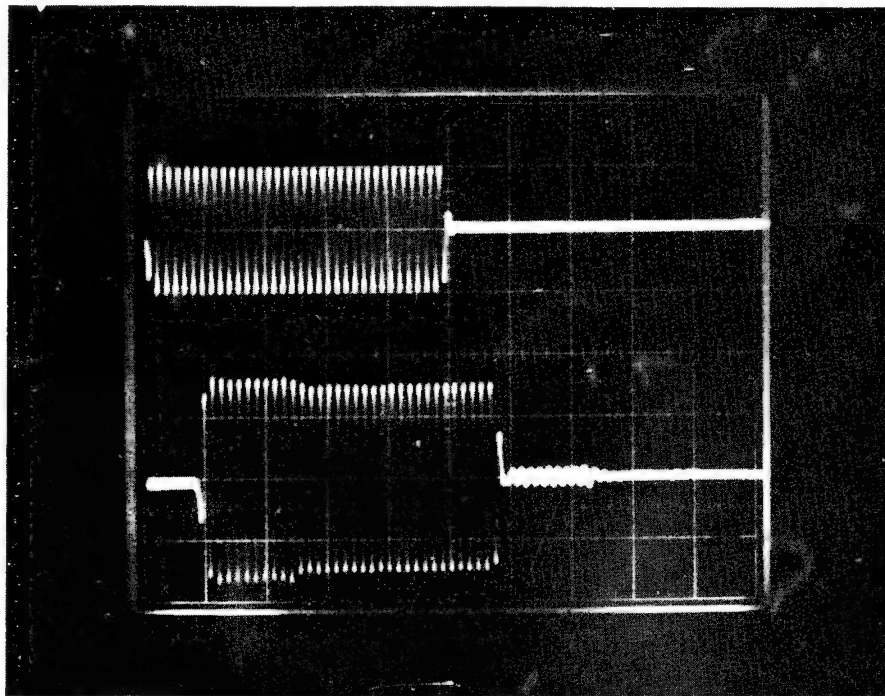 x_2 direction.

Fig. 8   Product of transduction ratios $F_1(\omega)F_2(\omega)$ for composite x_2 direction in test system.

Top trace: Input signal to the transmitting transducer
              Scale = 5v/Large Div.
              (The signal was attenuated 29dB before
              displaying.)

Bottom trace: Output signal from the receiving transducer
               Scale = 0.2v/Large Div.

Time scale: 5μs/Large Div.

Frequency: 1.2 MHz

Fig. 9   Typical ultrasonic through-transmission output
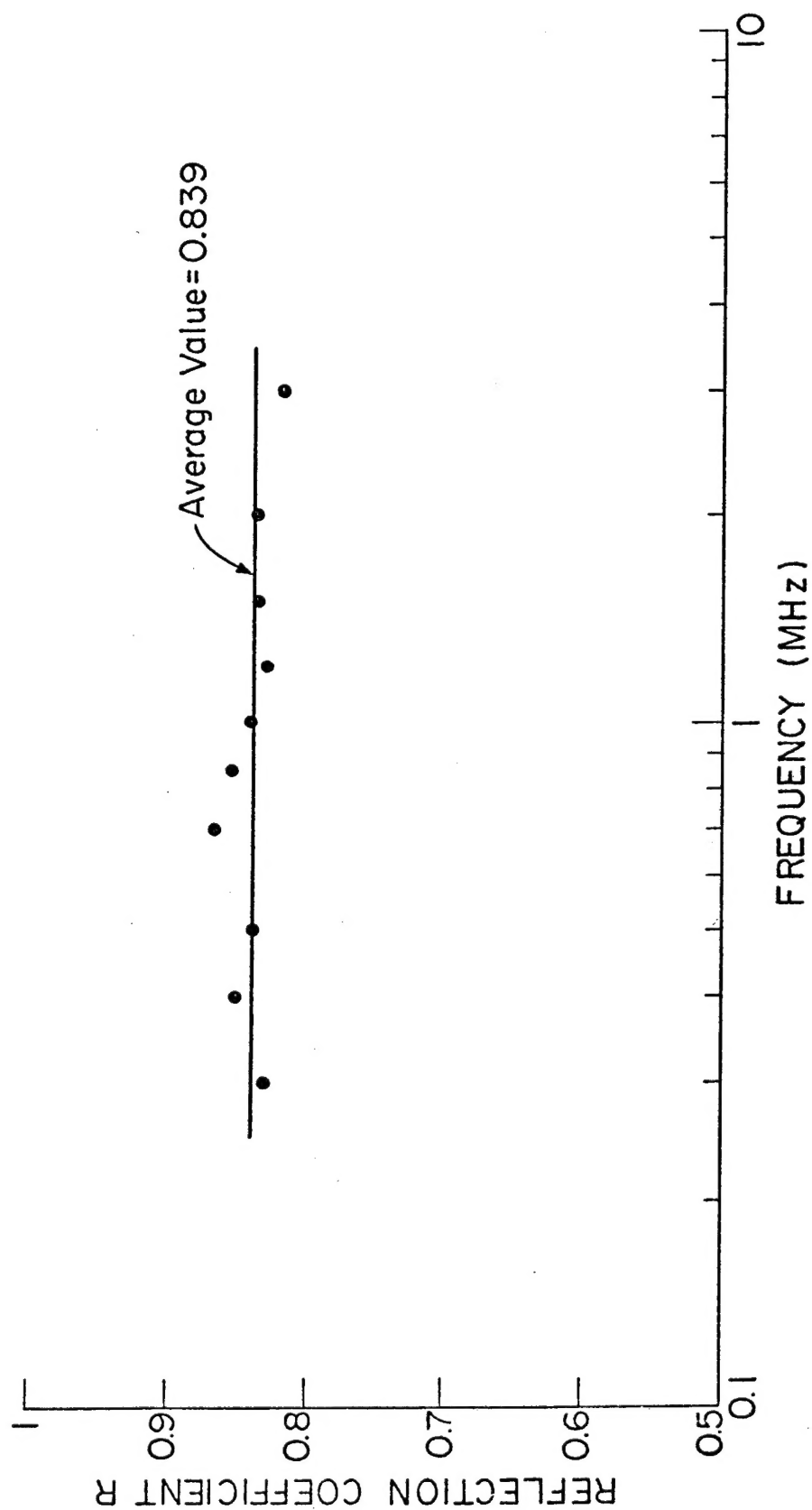   signal illustrating first reflection.

Fig. 10   Reflection coefficient R(ω) of stress waves in composite x_2 direction in test system.
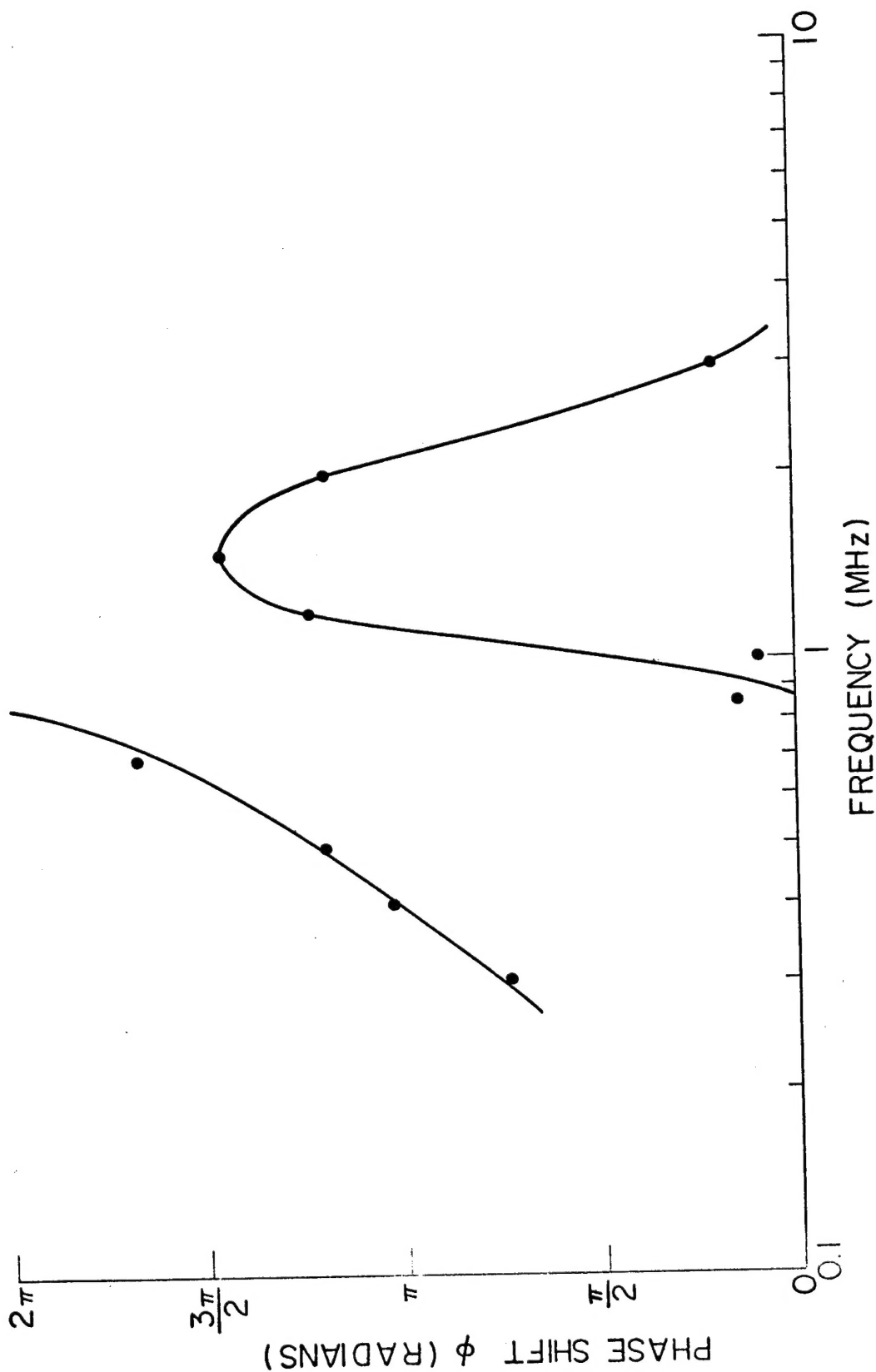
28

Fig. 11   Phase shift parameter $\phi(\omega)$ of stress waves in composite x_2 direction in test system.

E-242

29

1. Report No.	2. Government Accession No.	3. Recipient's Catalog No.
NASA CR-3203		

4. Title and Subtitle		5. Report Date
STRESS WAVE ATTENUATION IN THIN STRUCTURES BY ULTRASONIC THROUGH-TRANSMISSION		January 1980
		6. Performing Organization Code

7. Author(s)		8. Performing Organization Report No.
Samson S. Lee and James H. Williams, Jr.		None
		10. Work Unit No.

9. Performing Organization Name and Address		11. Contract or Grant No.
Massachusetts Institute of Technology Cambridge, Massachusetts 02139		NSG-3210
		13. Type of Report and Period Covered

12. Sponsoring Agency Name and Address		Contractor Report
National Aeronautics and Space Administration Washington, D.C. 20546		14. Sponsoring Agency Code

15. Supplementary Notes

Final report. Project Manager, Alex Vary, Materials and Structures Division, NASA Lewis Research Center, Cleveland, Ohio 44135.

16. Abstract

The steady-state amplitude of the output of an ultrasonic through-transmission measurement is analyzed and the result is given in closed form. Provided that the product of the input and output transduction ratios; the specimen-transducer reflection coefficient; the specimen-transducer phase shift parameter; and the material phase velocity are known, this analysis gives a means for determining the through-thickness attenuation of an individual thin sample. Multiple stress wave reflections are taken into account and so signal echoes do not represent a difficulty. An example is presented for a graphite fiber epoxy composite (Hercules AS/3501-6). Thus, the technique provides a direct method for continuous or intermittent monitoring of through-thickness attenuation of plate structures which may be subject to service structural degradation.

17. Key Words (Suggested by Author(s))	18. Distribution Statement
Ultrasonics; Ultrasonic attenuation; Non-destructive testing; Composites; Quality control and reliability	Unclassified - unlimited STAR Category 71

19. Security Classif. (of this report)	20. Security Classif. (of this page)	21. No. of Pages	22. Price*
Unclassified	Unclassified	30	A03